Measurement 272 (2026) 121098

Contents lists available at ScienceDirect

Measurement

journal homepage: www.elsevier.com/locate/measurement

Extended reality head-mounted displays as measuring systems: Conceptualization and measurement uncertainty evaluation

Leopoldo Angrisani [a], Egidio De Benedetto [a,*], Luigi Duraccio [a], Fabrizio Lo Regio [a], Michele Sansone [b], Annarita Tedesco [c]

[a] University of Naples Federico II - Department of Information Technology and Electrical Engineering, Naples, Italy
[b] University of Bari Aldo Moro, Department of Precision and Regenerative Medicine and Ionian Area - Section of Engineering, Bari, Italy
[c] University of Naples Federico II - Department of Public Health, Naples, Italy

ARTICLE INFO

Keywords:
Augmented reality
Extended reality
GUM
Measurements
Measurement system
Measurement uncertainty
Mixed reality
Industry 5.0
Metrological characterization
VIM
Virtual reality

ABSTRACT

This paper aims to conceptualize eXtended Reality Head-Mounted Displays (XR HMDs) as measuring systems. In fact, XR HMDs are commonly employed to integrate the physical and digital worlds by overlaying digital information onto the surrounding environment or enabling interactions with it, thereby providing immersive user experiences. When information originates from environment-related physical quantities, it is typically acquired through external measuring systems, with XR HMDs acting merely as a visualization device.

However, the availability of advanced onboard sensors and computational units has opened the possibility of reshaping the role of XR HMDs in the measurement processes. In this regard, much of the existing literature focuses on measurement algorithms embedded within XR HMDs; on the other hand, limited attention has been dedicated to performance aspects from a metrological perspective, which are instead crucial for a comprehensive conceptualization of XR HMDs as proper measuring devices. Within this novel framework, a key distinguishing factor is that users wearing XR HMDs (who act as *measurement operators*), introduce additional metrological challenges, particularly concerning their impact on the overall measurement uncertainty, which are generally more straightforward to manage in conventional measurement scenarios. To illustrate this perspective, without losing generality, a case study on distance measurement using a commercial XR HMD is presented. The results demonstrate the potential of XR HMDs to serve as proper measuring systems, provided that their specific sources of measurement uncertainty are adequately identified, evaluated, and combined.

1. Introduction

Extended Reality (XR) has emerged as a key enabling technology, initially within the framework of *Industry 4.0* [1], and more recently as a cornerstone of the evolving *Industry 5.0* paradigm [2], reflecting its increasing relevance in both technological and human-centric innovation. By encompassing Virtual Reality (VR), Augmented Reality (AR), and Mixed Reality (MR) technologies, XR offers experiences that seamlessly blend the physical and digital worlds, marking a profound transformation across multiple domains, including not only industry but also healthcare and entertainment [3–6].

Among XR devices, Head-Mounted Displays (HMDs) represent a prominent category, as they enable the integration of physical and digital content while simultaneously offering immersive user experiences [7,8]. This capability is guaranteed thanks to dedicated hardware and software components that support the visualization of digital information, which may be (i) pre-defined or (ii) dynamically adapted in response to data collected from users and/or their surrounding environment. In this regard, sensor systems embedded in XR HMDs, such as RGB cameras, depth cameras, or Inertial Measurement Units (IMUs), play a pivotal role. For pre-defined content, these onboard sensors map the surrounding space and track user movements in order to ensure the accurate placement of the digital elements within the user's Field of View (FoV) [9]. Instead, for dynamically-adapted content, they also recognize the user's actions (*e.g.*, hand gestures [10], or eye and head movements [11]) and translate them into meaningful system responses: in this case, they function as Human–Machine Interfaces (HMIs) [12].

However, in cases when information is derived from environment-related physical quantities (*e.g.*, length, area, and volume of objects, as well as the velocity of objects moving within the FoV [13]), XR HMDs generally act solely as visualization devices, relying on data acquired through external measurement systems [14,15]. This practice underutilizes the sensing capabilities already embedded in modern XR

* Corresponding author.
E-mail address: egidio.debenedetto@unina.it (E. De Benedetto).

https://doi.org/10.1016/j.measurement.2026.121098
Received 9 November 2025; Received in revised form 9 February 2026; Accepted 8 March 2026
Available online 9 March 2026

HMDs, limiting the full exploitation of the measurement performance offered by their onboard sensor systems and overlooking the potential to reposition XR HMDs as active elements within the measurement chain. In this novel perspective, XR HMDs can be considered fully fledged measuring systems, capable not only of retrieving data but also of generating it autonomously or semi-autonomously, while the user wearing the XR HMD takes the role of the *measurement operator*. This aspect has not yet been fully explored in the literature, where only a limited number of XR HMD-based measurement attempts can be found [16–19]. In all cases, the primary focus is on proposing measurement algorithms implemented within XR HMDs, without addressing their performance from a metrological perspective. Specifically, two critical metrological considerations remain largely overlooked:

- Manufacturers typically do not provide information regarding calibration procedures or instrumental uncertainty associated with the embedded sensor systems. Information is generally limited to consumer-level metrics and lacks details on traceability and testing conditions.
- The operator represents a critical *element* of the overall measurement chain, directly influencing the measurement process. Neglecting operator-related effects, such as (i) variability in pose, temporal instability, and (ii) differences between operators, may lead to an incomplete uncertainty budget. Although such factors are partly acknowledged in the *Guide to the Expression of Uncertainty in Measurement* (GUM) [20], standardized methods for the evaluation and combination of these contributions are still lacking.

Based on these considerations, this paper proposes a novel methodology, compliant with the GUM principles, to address the uncertainty budget associated with XR HMDs used as measuring systems. The proper identification, evaluation, and combination of all relevant uncertainty components facilitate a more rigorous assessment of whether a given XR HMD meets the requirements imposed by a specific measurement context. To illustrate this approach, and without loss of generality, a case study on distance measurement is presented using the Microsoft HoloLens 2 as the XR HMD [21].

The paper is organized as follows. In Section 2, the basic concepts of measurement uncertainty are recalled, along with the problem statement. Then, Section 3 illustrates the novel framework of considering XR HMDs as a measuring systems. The case study with Microsoft HoloLens 2 is described in Section 4, while the obtained experimental results are discussed in Section 5. Finally, conclusions are drawn and future work is outlined.

2. Background and problem statement

XR HMDs encompass devices with substantially different perceptual and technological characteristics across modalities. Following the reality–virtuality continuum proposed by Milgram and Kishino [22], AR overlays virtual content onto the real world using optical or video see-through displays (OST/VST); MR enables a deeper integration between real and virtual elements, allowing spatial anchoring, occlusions, and physically coherent interactions; finally, VR provides full immersion in synthetic environments via opaque stereoscopic displays. These modalities are designed to serve different application goals and user experiences, and, as a consequence, XR HMDs may exhibit substantially different hardware architectures and system characteristics. Such design choices translate into different performance profiles in terms of tracking, latency, geometric consistency, and rendering behavior [23].

For reshaping the role of an XR HMD as a measuring system, these aspects must be carefully considered, along with (i) the identification of the sources of measurement uncertainty; (ii) how to evaluate them; and (iii) how to combine them following a GUM-compliant approach. Therefore, for comprehensiveness, it is useful to briefly recall the established model used for uncertainty evaluation, along with a discussion of the critical issues that arise when the operator becomes a non-negligible influence factor in the measurement chain.

2.1. Fundamentals of uncertainty evaluation

As outlined in the *International Vocabulary of Metrology* (VIM), a measurement is *"a process of experimentally obtaining one or more quantity values, that can reasonably be attributed to a quantity"* [24]. To perform the measurement, a measuring system is needed, defined as *"a set of one or more measuring instruments which are assembled and adapted to give information used to generate measured quantity values within specified intervals for quantities of specified kinds"* [24].

All the quantities known to be involved in a measurement are comprised in the measurement model, namely the model relating the measurand (Y) and a set of N input quantities $\{X_i\}_{i=1}^{N}$. The measurement model is typically constituted by a functional relationship [24]:

$$Y = f(X_1, X_2, \dots, X_N) \tag{1}$$

The measurement result is typically expressed as (i) a *measured quantity value*, representing the best estimate of the measurand, along with (ii) a corresponding *measurement uncertainty*, namely a *"non-negative parameter characterizing the dispersion of the quantity values being attributed to a measurand, based on the information used"* [24], and (iii) the measurement unit. According to the GUM [20], the best estimate of the measurand $\overline{y}$ is obtained from the best estimates of the input quantities as expressed by

$$\overline{y} = f(\overline{x}_1, \overline{x}_2, \dots, \overline{x}_N) \tag{2}$$

This method is well established and allows for obtaining an unbiased estimate [25]. However, the evaluation of measurement uncertainty requires more in-depth considerations. In particular, three main sources of measurement uncertainty are conventionally recognized [26]:

1. *Definitional uncertainty*: it arises from the *"finite amount of detail in the definition of a measurand"* [24]. It may originate from an imperfect specification of the measurand or from an inaccurate definition of the interaction between the measurand and its environment. Since the identification and modeling phases are preliminary to any measurement activity and influence all subsequent steps, definitional uncertainty constitutes the *lower bound* of measurement uncertainty [27].
2. *Interaction uncertainty*: it arises from an imperfect or incomplete description of the interaction between the measurand and the measuring system to which it is connected. In fact, when a measuring system is connected to the measurand, an interaction occurs that may alter the measurand value during the measurement process. This phenomenon is also referred to as the *loading effect*. Since the origin of this contribution lies in the description and modeling phases, it can be regarded as a form of *definitional uncertainty*. For this reason, *interaction uncertainty* is not explicitly defined in the VIM [27]. Nonetheless, the interaction between the measurand and the measuring system is often sufficiently significant that the corresponding contribution to uncertainty is typically considered separately from other uncertainty components.
3. *Instrumental uncertainty*: it arises from the measuring system in use. Typically provided in the instrument specifications, it may result from the finite resolution of the system, approximations inherent in the measurement method and procedure, and the calibration of the system itself [24].

According to the GUM and the VIM, the *definitional uncertainty* component can be reduced by appropriately choosing the measurement model [20,24]. Similarly, *interaction uncertainty* can be minimized by designing an experimental procedure in which the disturbance introduced to the measurand is negligible. Once such conditions are achieved, the most significant component of measurement uncertainty is represented by *instrumental uncertainty*. For the sake of clarity, this conceptual structure is illustrated in Fig. 1. Overall, these considerations constitute a commonly acknowledged framework that encompasses the majority of measurement operations.

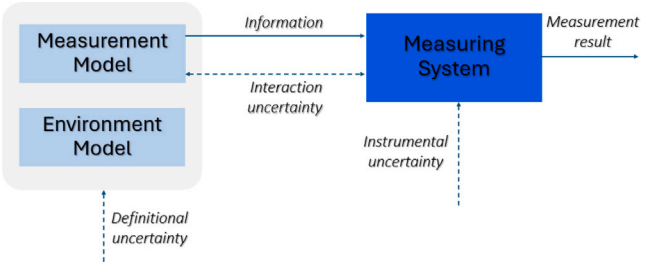

Fig. 1. Conventional components of Measurement Uncertainty.

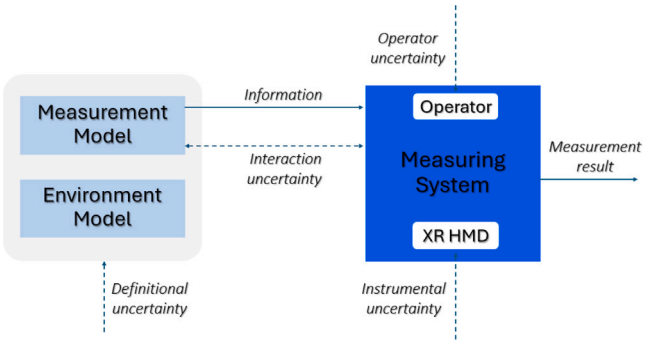

Fig. 2. Revised model of measurement uncertainty components.

2.2. Problem statement

The conceptual structure described in the previous section inherently includes an ideality condition related to the effects arising from one or more operators conducting the measurement. In this regard, part 6 of the GUM [28] refers to *manpower effects* to indicate sources of accidental errors such as incorrect measurement procedures, operator fatigue, and distraction. The same document also introduces the concept of *poorly understood effects*, which include, among others, those arising from different operators performing the same measurement. Overall, both *manpower* and *poorly understood* effects are recognized as contributing to the dispersion of values that can be attributed to the measurand and therefore should be explicitly addressed in the uncertainty analysis. However, in conventional measurement setups, these effects can typically be minimized with relative ease; for this reason, the GUM does not prescribe specific guidelines for addressing them.

Nevertheless, when XR HMDs are used as measuring systems, these effects can no longer be automatically neglected in the overall uncertainty budget; hence, the conventional approach can become insufficient. Even a single operator, fully aware of the measurement task and unaffected by fatigue, may introduce involuntary movements that alter the FoV of the XR HMD. Moreover, different operators naturally exhibit varying physical characteristics that can affect the positioning of the XR HMD relative to the measurand. In both cases, such operator-dependent effects ultimately influence the measurement result. Based on these considerations, it becomes necessary to introduce an additional uncertainty component, which can be referred to as *operator uncertainty*, accounting for these specific sources of variability.

3. Conceptualization of XR HMDs as measuring systems

To consider XR HMDs as fully fledged measuring systems, the conceptual structure of measurement uncertainty components should be revised to explicitly include *operator uncertainty*. In fact, the human operator becomes a significant element of the measurement chain: their actions and physical characteristics influence the measurement process in a non-negligible manner, extending beyond mere accidental effects due to fatigue or lack of familiarity with the measurement procedure to be conducted. Moreover, this additional uncertainty component should be properly evaluated and combined with the existing components in a manner consistent with the established uncertainty evaluation practices outlined in the GUM.

To this end, the following section introduces a novel framework specifically designed to address this issue.

3.1. Revised uncertainty model

Fig. 2 shows a sketch of the proposed, revised model of the measurement uncertainty components. The measurement and environment models remain unchanged, as the identification and modeling of the measurand constitute preliminary phases of any measurement activity and are subject only to *definitional uncertainty*. Therefore, neither the *measurement model* nor the *environment model* requires redefinition.

Instead, the *measuring system* block is expanded to address the operator-related effects. The measuring system is now considered to consist of two elements, namely the *XR HMD* (equipped with sensor systems) and the *operator*, with each contributing distinctly to the *interaction uncertainty*. However, it is worth noting that, within the considered framework of XR HMDs used to measure environment-related quantities, measurements are performed using non-contact sensing methods. Consequently, the physical value of the measurand remains unaffected by the presence of the operator or the XR HMD: therefore, *interaction uncertainty* can be considered negligible.

As in the conventional model, the XR HMD is subject to *instrumental uncertainty*, while the novel concept of *operator uncertainty* pertains to the human operator. As previously mentioned, the *operator uncertainty* component should be (i) evaluated to quantify the operator's influence on the measurement result,[1] and (ii) combined with the other uncertainty components, such as the *instrumental uncertainty* one.

3.2. Proposed uncertainty evaluation

Clearly, a necessary condition for conducting a thorough uncertainty evaluation is the identification of the measurand Y, the input quantities $\{X_i\}_{i=1}^{N}$, and the establishment of an appropriate measurement model $Y = f(X_1, X_2, \ldots, X_N)$. These elements are essential for the development and deployment of a dedicated application on the XR HMD used as a measuring system. Subsequently, the proposed method for uncertainty evaluation consists of three main steps, which should be carried out under controlled environmental conditions. For example, ambient illuminance is particularly critical in XR applications, as the visibility and clarity of digital content strongly depend on adequate illumination levels in the surrounding environment [29]. More generally, non-standard environmental conditions may lead to performance degradation or sensor drift [30], highlighting the importance for practitioners to ensure that XR HMDs operate within the limits specified by the manufacturer. The three-step method is described as follows.

1. The first step consists of conducting a conventional calibration procedure, with the XR HMD in a static configuration (*i.e.*, not worn by the operator). According to the VIM, calibration is defined as the *"operation that, under specified conditions, establishes a relation between the quantity values with measurement uncertainties provided by measurement standards and corresponding indications with associated measurement uncertainties"* [24]. Hence,

[1] In practice, the operator may affect the measurement result due to factors such as visual occlusions, imperfect alignment between virtual and physical objects, limitations in depth perception, latency-related effects, natural and involuntary body movements, or variability in the operator's height.

for a given reference quantity value y_{ref}, multiple indication values are acquired to obtain the best estimate of the measurand $\overline{y}_{\text{instr}}$, along with the corresponding measurement uncertainty, typically expressed as a standard uncertainty $u_{\text{instr}}(y)$, which represent the *instrumental uncertainty* component. Moreover, for each reference quantity value y_{ref}, this procedure allows for the estimation of the measurement error $e_{\text{instr}}(y)$, obtained as the difference between the best estimate $\overline{y}_{\text{instr}}$ and the reference value y_{ref} as $e_{\text{instr}}(y) = \overline{y}_{\text{instr}} - y_{\text{ref}}$. Overall, this procedure enables the identification of systematic effects and the evaluation of the *instrumental uncertainty*. It is important to note, however, that this procedure may not be feasible or meaningful in specific scenarios, such as measurements that necessarily require the operator to wear the XR HMD to perform an action (*e.g.*, the selection of points using hand gestures) [31].

2. Once the *instrumental uncertainty* has been evaluated, the second step addresses the variability of the indications that occurs when the XR HMD is worn by a single operator. This variability, also referred to as *within-operator* variability, is a contribution to the overall *operator uncertainty*, which arises from the interaction between the single operator and the XR HMD during the measurement process. The evaluation of such *within-operator* variability can be conducted in the same way as in step #1, with the only difference being that the XR HMD is now worn by the operator. Consequently, at the end of step #2, it is possible to obtain, for each reference quantity value y_{ref}, a best estimate $\overline{y}_{\text{within}}$, a standard uncertainty $u_{\text{within}}(y)$, and a measurement error $e_{\text{within}}(y) = \overline{y}_{\text{within}} - y_{\text{ref}}$. Unlike step #1, the obtained standard uncertainty accounts not only for the *instrumental uncertainty* component, but also for the contribution due to *within-operator* variability.
3. As aforementioned, each operator may exhibit different physical characteristics that influence the measurement result; hence, it is also necessary to evaluate the *between-operator* variability as an additional contribution to the overall *operator uncertainty*. The procedure is described as follows. For a given reference quantity value y_{ref}, repeated indications must be obtained from a cohort of M different operators. In this way, for each ith operator ($i = 1, 2, \ldots, M$), a best estimate $\overline{y}_{\text{within}^i}$, a standard uncertainty $u_{\text{within}^i}(y)$, and a measurement error $e_{\text{within}^i} = \overline{y}_{\text{within}^i} - y_{\text{ref}}$ can be determined. Given the best estimates vector from the M operators, $\{\overline{y}_{\text{within}^i}\}_{i=1}^{M}$, the overall best estimate $\overline{y}_{\text{between}}$ can be obtained as its arithmetic mean. The *between-operator* variability $u_{\text{between}}(y)$ is then evaluated as its standard uncertainty and represents the dispersion of the best estimates attributable to differences among the operators conducting the measurements. Once both the *within-operator* and *between-operator* variabilities are obtained, the overall *operator uncertainty* can be derived using the law of total variance [32] expressed as

$$u_{\text{operator}}(y) = \sqrt{u_{\text{between}}(y)^2 + u_{\text{within}}(y)^2} \tag{3}$$

where $u_{\text{within}}(y)$ is computed as the mean of the *within-operator* uncertainty vector $\{u_{\text{within}^i}(y)\}_{i=1}^{M}$.

In a nutshell, the proposed procedure draws inspiration from the established calibration of measuring devices, extending it to account for the uncertainty contribution of the operator wearing the XR HMD and performing the measurement.

Overall, by including operator-related effects into the measurement uncertainty model, a more reliable evaluation of the measurement uncertainty can be achieved.

For the sake of example, let us consider the case of an operator wearing an XR HMD and obtaining a single indication value related to an environment-related quantity to be measured. If the XR HMD has been characterized according to the method described above, it becomes possible, even with a single indication value, to determine an interval of values that can be reasonably attributable to the measurand, meaning that all relevant sources of variability have been accounted for, including those from the measuring system itself as well as from the *within-operator* and *between-operator* variability.[2]

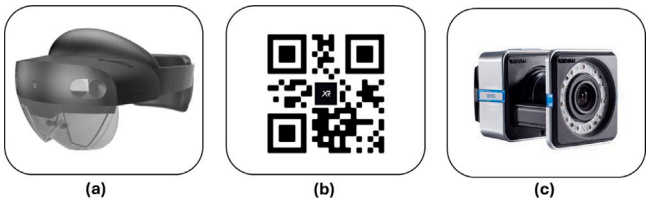

Fig. 3. Equipment chosen for the experimental setup: XR HMD Microsoft HoloLens 2 (a); QR code (b); and Vicon Vero camera (c).

4. Case study

As a case study for the applying the conceptualization proposed in Section 3, and without loss of generality, hands-free distance measurements were considered. Specifically, the following measurement scenario was identified: the operator wears the XR HMD, positions themselves in front of a wall featuring two reference points (represented by fiducial markers), and obtains indications from the XR HMD corresponding to the distance between the top-left corners of the two markers. Both the reference points and the wall belong to the *physical world*, hence the distance represents an environment-related quantity. Accordingly, the necessary equipment consists of: (i) the XR HMD worn by the operator, (ii) the fiducial markers from which the XR HMD derives the indications, and (iii) a reference system used to compare the measurement results obtained from the XR HMD. Overall, the selection of this specific case study was motivated by its relevance within the current literature, as highlighted in [34,35]. Nonetheless, to the best of the Authors' knowledge, there remains a lack of studies that formally conceptualize XR HMDs as fully fledged measuring systems by proposing a comprehensive method for evaluating all pertinent sources of uncertainty in accordance with the GUM guidelines.

It is worth mentioning that the proposed methodology is also applicable to the complementary case of marker-free distance measurements, relying on alternative interaction strategies, such as hand-based gestures [17] or the recognition of spatial anchors. In such scenarios, the marker-derived coordinates are simply substituted by spatial feature points identified by the HMD, maintaining the same formal approach for uncertainty evaluation.

4.1. Experimental setup

The equipment chosen for the experimental setup, shown in Fig. 3, is described as follows:

- *XR HMD*: The XR HMD chosen was Microsoft HoloLens 2. It is an OST XR HMD, characterized by a stereoscopic vision system consisting of visible light and infrared (IR) cameras (used as depth sensors), along with an IMU to track user head position and orientation [21]. These on-board sensor systems allow HoloLens 2 to scan the environment and effectively conduct distance measurements without any significant latency [36]. Although the

[2] Notably, a similar approach can be found in the context of HMIs, where *intra-individual* and *inter-individual* variabilities are considered [33]. Although the law of total variance is likewise applied, it is important to highlight that, in the case of HMIs, the objective is not the measurement of environment-related quantities, but rather the acquisition and classification of diverse human actions. As a result, the conclusions drawn in that context fall outside the scope of the present work.

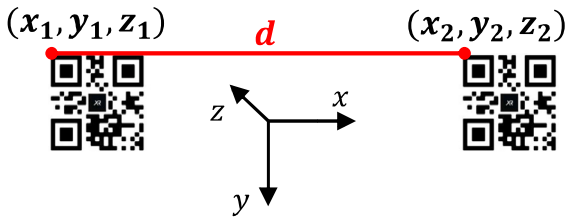

Fig. 4. Definition of the distance between two QR codes. The orientation of the *xyz* coordinate system follows the HoloLens 2 left-handed convention.

HoloLens 2 is a mature technological platform, its distinctive features continue to make it the most widely used OST HMD in current state-of-the-art applications [37]. Additionally, it is worth pointing out that, while the experimental setup focuses on this specific OST device, the proposed framework is designed to be platform-independent and is therefore also applicable to VST devices, such as the Meta Quest 3 [38] or Pico 4 [39], although the uncertainty sources would additionally need to account for the camera-mediated perception of the physical world. The XR environment was developed using the Unity game engine [40], integrating the Mixed Reality Toolkit (MRTK) [41] and the Microsoft.MixedReality.QR [42] libraries to enable the recognition of the fiducial markers. The implemented marker detection system provided detailed information regarding the spatial coordinates of the top-left corner of each marker.

- *Fiducial Markers*: The selected fiducial markers consisted of QR codes specifically designed to comply with the technical specifications of the HoloLens 2 device [42], as well as the requirements of XR applications in industrial and medical domains [35]. In particular, a set of custom QR codes with physical dimensions of 100 × 100 mm was employed [42]. Given two QR codes affixed to a surface, the distance between their top-left corners was evaluated through the measurement model shown in (4):

$$d = \sqrt{(x_1 - x_2)^2 + (y_1 - y_2)^2 + (z_1 - z_2)^2} \tag{4}$$

where the *z*-axis corresponds to depth, and the orientation of the *xyz* coordinate system follows the left-hand rule, as defined by the HoloLens 2 reference frame. Hence, the XR environment provides direct information on the coordinates of the QR codes, whereas the distance between the QR codes was determined indirectly through the application of the measurement model. Fig. 4 provides a representation of the measurand definition.

- *Reference system*: A high-performance motion capture system based on Vicon Vero [43] cameras, consisting of ten IR cameras, was used as the reference system. A series of reflective markers was used to evaluate the positions of the fiducial markers and measure the distances between their top-left corners as a ground-truth. Data were collected after the calibration procedure, performed according to the specifications recommended by the system manufacturer. The software used was Vicon Tracker [44].

The experimental setup was established in a controlled environment to ensure consistency with the technical and functional constraints of the selected equipment, while preserving the generalizability of the proposed method. In particular, ambient illuminance was identified as a critical environmental factor and was maintained within the optimal range recommended by Microsoft (specifically, [500-1000] lux [45]) to ensure reliable visualization of digital content and accurate recognition of QR codes [42]. Additionally, the ambient temperature was maintained within the interval [20–25] °C to prevent sensor drift and preserve the stability of the chosen equipment.

A representation of the setup is shown in Fig. 5. In particular, Fig. 5-(a) shows a general overview of the experimental setup (not to scale). Hence, Fig. 5-(b) shows seven QR codes affixed to a white wall, ensuring adequate contrast for reliable detection. All QR codes were positioned at fixed locations and aligned at a uniform height of $h = (155.0 \pm 0.1)$ cm above the floor level, measured using a tape measure.[3] QR code #0 established the origin of the coordinate system and remained active throughout the session, whereas the other six QR codes were revealed sequentially to represent $D = 6$ different distance values $\{d_j\}_{j=1}^{D}$ between the QR code #j and QR code #0.

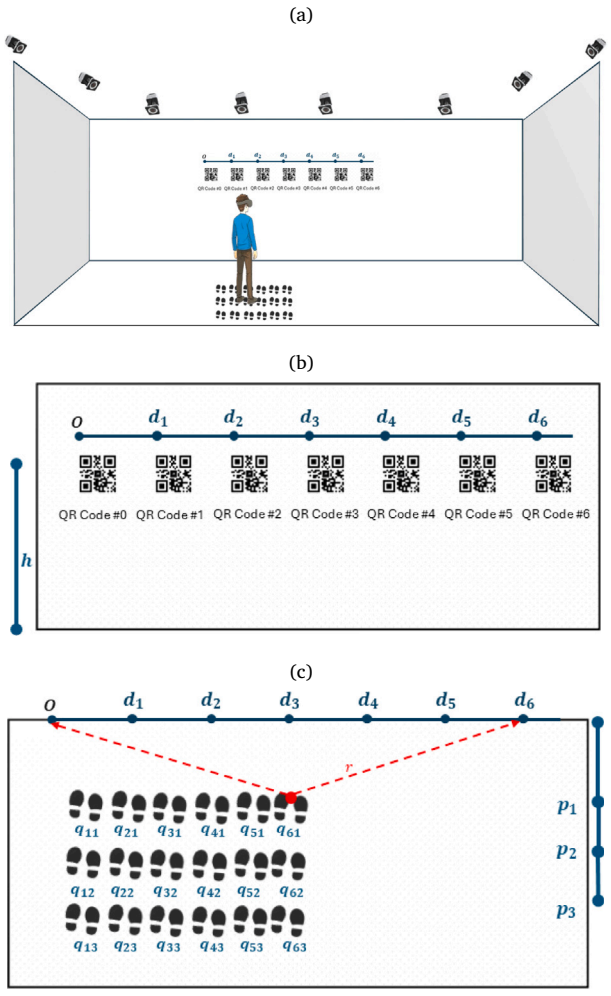

Fig. 5. Sketch of the experimental setup: (a) general overview (not to scale); (b) front view with the QR codes placed at a height *h*; (c) top view with the measurement points q_{ij} delineated on the floor to be equidistant from the QR codes between which the distance was to be measured.

As a preliminary step to the acquisition of experimental data via the Microsoft HoloLens 2, the Vicon system was employed to record the position of the reflective markers affixed to the top-left corner of each QR code. The reflective markers were placed at the top-left corners of each QR code to enable detection by the Vicon system, in order to obtain a corresponding reference value $\{d_{\mathrm{ref}_j}\}_{j=1}^{D}$ for each of the aforementioned distance $\{d_j\}_{j=1}^{D}$. Data acquisition was performed over a 10-second interval at a sampling rate of 100 samples per second (sps), yielding a total of 1000 indication values for each distance

[3] The use of a tape measure to provide information regarding the height at which the QR codes are positioned is only for indicative purposes, as the reference measurements of the distance between the QR codes were conducted using the Vicon Vero cameras.

$\{d_j\}_{j=1}^{D}$. The best estimates (evaluated as the mean values) and the corresponding percentage standard uncertainties, expressed in parts per million (ppm), for the each distances $\{d_j\}_{j=1}^{D}$ were determined through a Type-A evaluation [20], and are reported in Table 1.

Finally, Fig. 5-(c) depicts the different positions of the operator. Since, as already described, QR code #0 established the origin of the coordinate system and remained active throughout the session (whereas the other six QR codes were revealed sequentially to represent the different distances to be measured) six midpoints were marked horizontally on the floor, facilitating the correct alignment between the participants wearing the HoloLens 2 and the active QR codes and ensuring a consistent viewing angle for all participants. Moreover, three different depths (p), defined as the distances between the wall and the positions from which participants performed the measurements, were considered. The selected depth values, denoted as $\{p_k\}_{k=1}^{P}$ with $P = 3$, were $\{70.0, 90.0, 110.0\}$ cm, each determined with mm-scale uncertainty using a tape measure. These depth values were chosen following the official guidelines provided for Microsoft HoloLens 2 [46]. Hence, given the $D = 6$ distance values $\{d_j\}_{j=1}^{D}$ between QR codes and the $P = 3$ depth values $\{p_k\}_{k=1}^{P}$, a total of 18 measurement points were delineated on the floor. Specifically, each measurement point was denoted as q_{jk}, with $j = 1, \ldots, D$ and $k = 1, \ldots, P$ representing, respectively, the distance to be measured d_j and the depth p_k at which the user was positioned. This configuration ensured that each measurement point was equidistant from the QR codes used for distance measurement.

For the sake of example, the measurement point q_{16} was used to measure the distance d_6 between the QR codes #0 and #6, at a depth p_3. For this reason, it is positioned in the center between the QR code #0 and the QR code #6 to guarantee the same distance (denoted as r) to the two QR codes. At each of these points, a measurement operation was conducted with a fixed duration of 10 s, during which participants wearing Microsoft HoloLens 2 acquired $I = 30$ indication values. The total experimental session for each participant lasted approximately 15 min.

4.2. Flowchart of the experimental procedure

To better clarify the experimental procedure for acquiring measurement data, the following flowchart is provided.

1. First, the XR HMD is worn and the user is positioned at depth p_1 with respect to the wall. QR #0 remains uncovered throughout the entire experiment.
2. QR #1 is uncovered, and the user moves to position q_{11} to measure distance d_1.
3. QR #1 is then covered and QR #2 is uncovered. The user moves to position q_{21} to measure distance d_2.
4. This procedure is repeated sequentially for all remaining QR codes (up to QR #6), each time uncovering the next QR code, positioning the user at the corresponding location, and measuring the associated distance value $\{d_j\}_{j=1}^{D}$.
5. After completing the full set of distance measurements at depth p_1, the user steps back to depth p_2, where the entire measurement sequence is repeated.
6. Once the measurements at depth p_2 are completed, the same measurement cycle is finally performed at depth p_3.

In this way, for each user, 18 independent measurement results are obtained, corresponding to 6 distance values $\{d_j\}_{j=1}^{D}$ ($D = 6$) measured at each of the 3 depth values $\{p_k\}_{k=1}^{P}$ ($P = 3$).

4.3. Experimental campaign

The experimental campaign involved $M = 32$ healthy participants aged between 20 and 31 years. All participants had normal or corrected-to-normal vision and provided written informed consent prior to participation. Their heights ranged from 150 cm to 186 cm and were distributed as illustrated in the histogram shown in Fig. 6. Before conducting the experiments, all participants received clear instructions on the task to be performed (*i.e.*, to remain as still as possible during the measurements). Participants wore HoloLens 2, adjusting it to display the digital content correctly and performing eye calibration prior to starting the experiments in order to guarantee the stability of the holograms.

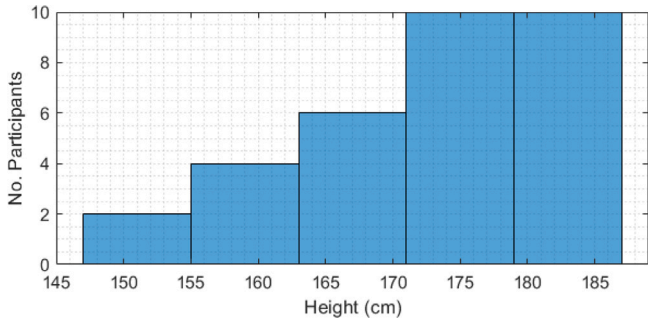

Fig. 6. Distribution of the participants' heights.

5. Experimental results

Following Step #1 of the proposed framework (described in Section 3.2), preliminary measurements were conducted with HoloLens 2 in a static configuration (*i.e.*, placed on a mannequin head), in order to (i) evaluate the instrumental uncertainty contribution and (ii) ensure that the device's baseline performance was quantified independently of human-induced variability. Then, for each measurement point, characterized by specific distance between QR codes $\{d_j\}_{j=1}^{D}$ and depth $\{p_k\}_{k=1}^{P}$, a total of $I = 30$ indication values were obtained for each of the $M = 32$ participants. Hence, for each distance, depth, and participant, the best estimate (as the arithmetic mean among the indications) and the standard uncertainty (through a type-A evaluation) were evaluated. Therefore, for each distance and depth, the results for each participant were combined through the law of total variance expressed by (3), in order to obtain a combined standard uncertainty which considers both the *within-operator* and the *between-operator* contribution to the *operator uncertainty*.

The obtained results are summarized in Table 2, where the measurement result is reported in terms of mean value (mm) and combined standard uncertainty (%), expressed as a percentage. Additionally, in the last row, the measurement results were further aggregated across all considered depths $\{p_k\}_{k=1}^{P}$ to provide a representative uncertainty specification over a broader range of operational depths. Moreover, Table 3 reports the measurement error $\{e_j\}_{j=1}^{D}$, expressed as a percentage, between the reference quantity values provided by the Vicon system and the measured quantity values provided by the operators wearing HoloLens 2, for each condition reported in Table 2.

5.1. Discussion

The conducted preliminary tests in static configuration revealed that the instrumental uncertainty component of HoloLens 2 was negligible compared to the operator-induced variability. Therefore, the following analysis focuses directly on *within-* and *between-operator* variability.

Table 2 reveals a decreasing measurement uncertainty as the distance between QR codes increases. This behavior could be attributed to the intrinsic features of HoloLens 2. When the distances to be measured cover a significant area, close to the full FoV, the device employs a higher spatial information density, namely a larger number of pixels. In these conditions, any detection errors on single pixels have a lower

Table 1
Distances between the QR code #j and QR code #0, measured by Vicon tracker in terms of mean values (mm) and percentage uncertainty (ppm).

Distance between the QR codes - Vicon results (mm)					
d_{ref_1}	d_{ref_2}	d_{ref_3}	d_{ref_4}	d_{ref_5}	d_{ref_6}
149.772 (17 ppm)	299.377 (39 ppm)	448.117 (5 ppm)	599.028 (4 ppm)	747.637 (3 ppm)	898.968 (3 ppm)

Table 2
Mean value (mm) and relative standard uncertainty (%) measured through HoloLens 2 for each distance between QR codes and each projected depth. The obtained standard uncertainty is evaluated considering both *within-operator* and *between-operator* variability following the proposed method described in Section 3.

Depth ↓	Distance between the QR codes - HoloLens 2 results (mm) →					
	d_{meas_1}	d_{meas_2}	d_{meas_3}	d_{meas_4}	d_{meas_5}	d_{meas_6}
p_1	150.9 (2.0%)	299.7 (1.4%)	449.6 (1.0%)	601.6 (0.9%)	750.7 (0.7%)	899.8 (0.9%)
p_2	150.8 (1.9%)	299.9 (1.2%)	449.8 (0.9%)	601.9 (1.1%)	750.7 (1.0%)	900.1 (1.0%)
p_3	150.8 (2.6%)	300.0 (1.3%)	449.8 (1.2%)	602.4 (0.9%)	751.0 (1.0%)	900.2 (0.9%)
Combined	150.8 (2.2%)	299.9 (1.3%)	449.7 (1.0%)	602.0 (0.9%)	750.8 (0.9%)	900.0 (0.9%)

Table 3
Measurement error (expressed as a percentage) between measured and reference values.

Depth ↓	Measurement Error (%)					
	e_1	e_2	e_3	e_4	e_5	e_6
p_1	0.76%	0.10%	0.33%	0.43%	0.41%	0.09%
p_2	0.75%	0.17%	0.38%	0.48%	0.40%	0.13%
p_3	0.74%	0.21%	0.37%	0.56%	0.45%	0.13%
Combined	0.75%	0.16%	0.36%	0.49%	0.42%	0.12%

impact on the overall precision of the measurement. In addition, measurement errors shown in Table 3 reveal a significantly low deviation between the measured quantity values provided by HoloLens 2 and those provided by the Vicon system, suggesting a good accuracy of the XR HMD.

Furthermore, the analysis of *within-* and *between-operator* variability revealed a significant difference between the two contributions, showing a greater influence of the *between-operator* contribution for each of the 18 measurement points. This outcome suggests that the main sources of variability may not be attributed to the performance of the measuring system itself (*i.e.*, the *instrumental uncertainty*), but rather to the intrinsic and behavioral characteristics of the operator. As such, by considering participant height as a potential influencing factor, statistical analyses on the measurement results obtained by each operator, in terms of mean value and *within-operator* variability, were conducted. In particular, for each distance between the QR codes $\{d_j\}_{j=1}^{D}$ and depth $\{p_k\}_{k=1}^{P}$, linear correlation analysis between the participant heights and the associated measurement uncertainty values was carried out through the evaluation of Pearson's correlation coefficients. However, the obtained correlation coefficient values $\{0.19, 0.15, 0.20\}$ suggested low correlation, *i.e.*, it is not possible to state that the measurement uncertainty increases or decreases as a function of the participants' height.

In conclusion, although the overall measurement uncertainty is predominantly influenced by the *between-operator* rather than the *within-operator* variability, it is not possible to assert that the primary source of variability is the participants' height. This implies that the HoloLens 2 is robust with respect to this specific source of variability. Therefore, a possible explanation for the significant between-operator variability may be the physiological micro-movements exhibited during measurement tasks, the analysis of which would require data from IMUs embedded in the XR HMD.

6. Conclusions and future work

This work addressed the novel perspective of employing XR HMDs not merely as visualization tools, but as active measuring systems capable of providing information about environment-related physical quantities. Specifically, a novel methodology was proposed for the evaluation of the measurement uncertainty associated with XR HMDs, in accordance with the principles of the Guide to the Expression of Uncertainty in Measurement (GUM). The approach was developed through the identification of all relevant uncertainty sources, distinguishing between the contributions due to the XR HMD itself (*instrumental uncertainty*), those arising from the same operator wearing the HMD (*within-operator* variability), and those related to the variability among different operators (*between-operator* variability). A structured methodology, based on a three-step procedure conducted under controlled conditions, was outlined to systematically evaluate and combine these components.

A marker-based distance measurement scenario using Microsoft HoloLens 2 was selected as a case study, due to its relevance in both industrial and medical applications. The experimental campaign, involving a cohort of 32 healthy participants, demonstrated the effectiveness of the proposed framework in evaluating the overall measurement uncertainty. While the *between-operator* variability emerged as the dominant contribution, the analysis did not reveal a significant correlation between participants' height and measurement uncertainty, suggesting robustness of HoloLens 2 with respect to this potential source of variability. The results rather indicate that minor, individual-specific micromovements might be responsible for the observed uncertainty.

In summary, the proposed methodology enables a comprehensive and GUM-compliant uncertainty evaluation for XR-based measurements, ensuring traceability and reliability of the indications provided by the XR HMD. Furthermore, it offers a structured means to identify the most critical contributions to uncertainty for any given measurement scenario, thereby guiding possible mitigation strategies aimed at enhancing the metrological performance of XR HMDs when used as active measurement systems. Importantly, considering the human factor in the form of operator-related effects allows advancing towards a more human-centric perspective, aligning with one of the pillars of the *Industry 5.0* paradigm. In future work, influencing factors such as ambient illuminance, temperature, and operator-related conditions (*e.g.*, fatigue) will be investigated, together with possible strategies to mitigate these effects, including ergonomic supports, training protocols, and algorithmic compensation. In addition, the applicability of the approach to markerless measurements will also be explored. Such an analysis will be instrumental in assessing the applicability of XR HMDs across a broader range of measurement tasks, especially in dynamic and unstructured environments where marker deployment may not be feasible. The results are expected to provide further insight into the metrological implications of different localization and tracking strategies, thus contributing to the development of generalized uncertainty evaluation frameworks for XR-based measurement systems.

CRediT authorship contribution statement

Leopoldo Angrisani: Writing – review & editing, Resources, Project administration, Funding acquisition, Conceptualization. **Egidio De Benedetto:** Writing – review & editing, Supervision, Methodology, Formal analysis, Conceptualization. **Luigi Duraccio:** Writing – original draft, Supervision, Methodology, Formal analysis, Conceptualization. **Fabrizio Lo Regio:** Writing – original draft, Visualization, Validation, Software, Investigation, Data curation. **Michele Sansone:** Writing – original draft, Visualization, Validation, Software, Investigation, Data curation. **Annarita Tedesco:** Writing – review & editing, Supervision, Methodology, Formal analysis, Conceptualization.

Declaration of competing interest

The authors declare that they have no known competing financial interests or personal relationships that could have appeared to influence the work reported in this paper.

Acknowledgment

This work was financially supported by the Italian Ministry of University and Research (MUR) through the projects "RESearch and innovation on future Telecommunications systems and networks - RESTART", PNRR PE14 (CUP E63C22002040007); "Made in Italy Circolare e Sostenibile", PNRR PE11 (CUP E63C22002130007).

Data availability

Data will be made available on request.

References

[1] P. Daponte, L. De Vito, F. Picariello, M. Riccio, State of the art and future developments of the augmented reality for measurement applications, Measurement 57 (2014) 53–70.

[2] H. Yang, P. Wang, R. Luo, S. Zhao, Y. Zhang, Evaluating the effectiveness and usability of SAR-based inspection application for product quality, Measurement 256 (2025) 118293, http://dx.doi.org/10.1016/j.measurement.2025.118293, URL https://www.sciencedirect.com/science/article/pii/S0263224125016525.

[3] P. Cipresso, I.A.C. Giglioli, M.A. Raya, G. Riva, The past, present, and future of virtual and augmented reality research: a network and cluster analysis of the literature, Front. Psychol. 9 (2018) 2086.

[4] A.Y. Yiğit, M. Uysal, Virtual reality visualisation of automatic crack detection for bridge inspection from 3D digital twin generated by UAV photogrammetry, Measurement (2025) 115931.

[5] M. Żuk, M. Wojtków, M. Popek, J. Mazur, K. Bulińska, Three-dimensional gait analysis using a virtual reality tracking system, Measurement 188 (2022) 110627.

[6] A. Logeswaran, C. Munsch, Y.J. Chong, N. Ralph, J. McCrossnan, The role of extended reality technology in healthcare education: Towards a learner-centred approach, Futur. Heal. J. 8 (1) (2021) e79–e84.

[7] A. Alhakamy, Extended reality (XR) toward building immersive solutions: the key to unlocking industry 4.0, ACM Comput. Surv. 56 (9) (2024) 1–38.

[8] L. Chen, T. Qiu, L. Ma, W. Zhan, Y. Zhang, L. Sun, An augmented reality surgical navigation system based on co-axial projection of surgical paths for open liver tumor surgery, Measurement 235 (2024) 114991.

[9] L. Hwang, J. Lee, J. Hafeez, J. Kang, S. Lee, S. Kwon, A study on optimized mapping environment for real-time spatial mapping of HoloLens, Int. J. Internet, Broadcast. Commun. 9 (3) (2017) 1–8.

[10] L. Angrisani, M. D'Arco, E. De Benedetto, L. Duraccio, F. Lo Regio, M. Sansone, A. Tedesco, Performance measurement of gesture-based human–machine interfaces within eXtended reality head-mounted displays, Sensors 25 (9) (2025) 2831, http://dx.doi.org/10.3390/s25092831.

[11] L. Angrisani, M. D'Arco, E. De Benedetto, L. Duraccio, F. Lo Regio, A. Tedesco, A method for the metrological characterization of eye-and head-tracking interfaces for human–machine interaction through extended reality head-mounted displays, Measurement 243 (2025) 116279, http://dx.doi.org/10.1016/j.measurement.2024.116279.

[12] Y. Xin, K. Kam, L. Qinbiao, Y. Cho Yin, L. Chun Kit, F. Ka Hei, N. Lok Hei, Exploring the human-centric interaction paradigm: augmented reality-assisted head-up display design for collaborative human-machine interface in cockpit, Adv. Eng. Inform. 62 (2024) 102656.

[13] N. Neshov, A. Manolova, Objects distance measurement in augmented reality for providing better user experience, in: IOP Conference Series: Materials Science and Engineering, vol. 1032, (1) IOP Publishing, 2021, 012020.

[14] S. Doolani, C. Wessels, V. Kanal, C. Sevastopoulos, A. Jaiswal, H. Nambiappan, F. Makedon, A review of extended reality (XR) technologies for manufacturing training, Technologies 8 (4) (2020) 77.

[15] F. Beltrán, J. Geng, Building a distributed XR immersive environment for data visualization, in: 2021 ITU Kaleidoscope: Connecting Physical and Virtual Worlds (ITU K), IEEE, 2021, pp. 1–8.

[16] H.C. Gagnon, C.S. Rosales, R. Mileris, J.K. Stefanucci, S.H. Creem-Regehr, R.E. Bodenheimer, Estimating distances in action space in augmented reality, ACM Trans. Appl. Percept. (TAP) 18 (2) (2021) 1–16.

[17] H. Jing, Y. Boxiong, C. Jiajie, Non-contact measurement method research based on hololens, in: 2017 International Conference on Virtual Reality and Visualization, ICVRV, IEEE, 2017, pp. 267–271.

[18] M. Rousian, A. Koning, R. Van Oppenraaij, W. Hop, C. Verwoerd-Dikkeboom, P. Van Der Spek, N. Exalto, E. Steegers, An innovative virtual reality technique for automated human embryonic volume measurements, Hum. Reprod. 25 (9) (2010) 2210–2216.

[19] H.M.A. Mageed, I. Azzam, F. Breidi, State of electrical metrology and possible advancements utilizing extended reality, Mapan 40 (1) (2025) 151–163.

[20] I. BIPM, I. IFCC, I. ISO, O. IUPAP, Guide to the expression of uncertainty in measurement, JCGM 100: 2008 GUM 1995 with minor corrections, Jt. Comm. Guid. Metrol. 98 (2008).

[21] Microsoft Hololens 2, 2025, https://learn.microsoft.com/en-us/hololens/. (Accessed 11 March 2026).

[22] P. Milgram, F. Kishino, A taxonomy of mixed reality visual displays, IEICE Trans. Inf. Syst. 77 (12) (1994) 1321–1329.

[23] S.M. LaValle, Virtual Reality, Cambridge University Press, 2023.

[24] I. Vim, International vocabulary of metrology (VIM) - – basic and general concepts and associated terms (VIM), Int. Organ. 3rd edition (2008).

[25] W. Bich, M.G. Cox, P.M. Harris, Evolution of the 'guide to the expression of uncertainty in measurement', Metrologia 43 (4) (2006) S161.

[26] W. Bich, From errors to probability density functions. Evolution of the concept of measurement uncertainty, IEEE Trans. Instrum. Meas. 61 (8) (2012) 2153–2159.

[27] A. Ferrero, D. Petri, P. Carbone, M. Catelani, Modern Measurements: Fundamentals and Applications, John Wiley & Sons, 2015.

[28] I. BIPM, I. IFCC, I. ISO, O. IUPAP, Guide to the expression of uncertainty in measurement - part 6: Developing and using measurement models, Jt. Comm. Guid. Metrol. (2020).

[29] D. Kahl, M. Ruble, A. Krüger, The influence of environmental lighting on size variations in optical see-through tangible augmented reality, in: 2022 IEEE Conference on Virtual Reality and 3D User Interfaces, VR, IEEE, 2022, pp. 121–129.

[30] H.-J. Guo, J.Z. Bakdash, L.R. Marusich, B. Prabhakaran, Augmented reality and mixed reality measurement under different environments: A survey on head-mounted devices, IEEE Trans. Instrum. Meas. 71 (2022) 1–15.

[31] J.L. Raheja, M. Chandra, A. Chaudhary, 3D gesture based real-time object selection and recognition, Pattern Recognit. Lett. 115 (2018) 14–19.

[32] C.W. Champ, A.V. Sills, The generalized laws of total variance and total covariance, in: Southern Georgia Mathematics International Conference, Springer, 2021, pp. 243–254.

[33] L. Angrisani, M. D'Arco, E. De Benedetto, L. Duraccio, F.L. Regio, A. Tedesco, A novel measurement method for performance assessment of hands-free, XR-based human-machine interfaces, IEEE Sensors J. (2024) http://dx.doi.org/10.1109/JSEN.2024.3444472.

[34] G.M. Costa, M.R. Petry, J.G. Martins, A.P.G. Moreira, Assessment of multiple fiducial marker trackers on hololens 2, IEEE Access 12 (2024) 14211–14226.

[35] A. Florkowska, M. Trojak, W. Celniak, M. Stanuch, M. Daniol, A. Skalski, Metrological analysis of HoloLens 2 for visual marker-based surgical navigation, in: 2023 IEEE International Conference on Imaging Systems and Techniques, IST, IEEE, 2023, pp. 1–6.

[36] Microsoft Hololens 2 – Hardware Specifications, 2025, https://learn.microsoft.com/en-us/hololens/hololens2-hardware. (Accessed 11 March 2026).

[37] A. Palumbo, Microsoft HoloLens 2 in medical and healthcare context: state of the art and future prospects, Sensors 22 (20) (2022) 7709.

[38] Meta Quest 3, 2023, https://www.meta.com/quest/quest-3/. (Accessed 02 February 2026).

[39] PICO 4, 2022, https://www.picoxr.com/it/products/pico4. (Accessed 02 February 2026).

[40] Unity, 2025, https://unity.com/ . (Accessed 11 March 2026).

[41] Mixed Reality Toolkit, 2025, https://learn.microsoft.com/en-us/windows/mixed-reality/mrtk-unity/mrtk2/?view=mrtkunity-2022-05. (Accessed 11 March 2026).

[42] QR code Detection Overview, 2025, https://learn.microsoft.com/it-it/windows/mixed-reality/develop/advanced-concepts/qr-code-tracking-overview. (Accessed 11 March 202609 November 2025).

[43] The vicon vero - compact super wide camera, 2025, https://www.vicon.com/hardware/cameras/vero/. (Accessed 09 November 2025).
[44] Vicon tracker system components, 2025, https://help.vicon.com/space/Tracker39/14059373/Tracker+system+components. (Accessed 09 November 2025).
[45] Hololens environment considerations, 2025, https://learn.microsoft.com/it-it/hololens/hololens-environment-considerations. (Accessed 09 November 2025).
[46] Best practices for QR code detection, 2025, https://learn.microsoft.com/en-us/windows/mixed-reality/develop/advanced-concepts/qr-code-tracking-overview#best-practices-for-qr-code-detection. (Accessed 09 November 2025).